nature plants

LETTERS

PUBLISHED: 27 APRIL 2015 | ARTICLE NUMBER: 15053 | DOI: 10.1038/NPLANTS.2015.53

The plasticity of cyanobacterial metabolism supports direct CO_2 conversion to ethylene

Wei Xiong[1], John A. Morgan[2], Justin Ungerer[1], Bo Wang[1], Pin-Ching Maness[1] and Jianping Yu[1]*

The cyanobacterial tricarboxylic acid (TCA) cycle functions in both in biosynthesis and energy generation. However, it has until recently been generally considered to be incomplete[1,2] with limited flux[3,4], and few attempts have been made to draw carbon from the cycle for biotechnological purposes. We demonstrated that ethylene can be sustainably and efficiently produced from the TCA cycle of the recombinant cyanobacterium *Synechocystis* 6803 expressing the *Pseudomonas* ethylene-forming enzyme (Efe)[5]. A new strain with a modified ribosome binding site upstream of the *efe* gene diverts 10% of fixed carbon to ethylene and shows increased photosynthetic activities. The highest specific ethylene production rate reached 718 ± 19 μl l^{-1} h^{-1} per $A_{730\,nm}$. Experimental and computational analyses based on kinetic ^{13}C-isotope tracer and liquid chromatography coupled with mass spectrometry (LC–MS) demonstrated that the TCA metabolism is activated by the ethylene forming reaction, resulting in a predominantly cyclic architecture. The outcome significantly enhanced flux through the remodelled TCA cycle (37% of total fixed carbon) compared with a complete, but bifurcated and low-flux (13% of total fixed carbon) TCA cycle in the wild type. Global carbon flux is redirected towards the engineered ethylene pathway. The remarkable metabolic network plasticity of this cyanobacterium is manifested by the enhancement of photosynthetic activity and redistribution of carbon flux, enabling efficient ethylene production from the TCA cycle.

Engineering photosynthetic organisms offers an attractive approach to couple carbon sequestration to the production of fuels and chemicals[6,7]. Initial efforts to improve photosynthetic productivity involved heterologous expression of pathway enzymes. However, high productivity of a target metabolite requires significant redirection of flux in primary metabolism which may not readily occur, depending on the flux redistribution at branch nodes controlled by the rigidity of the metabolic network[8]. To date, the rigidity versus flexibility of phototrophic metabolism remains largely unknown, due to the paucity of model phototrophs with significantly altered carbon fluxes, and the lack of high-resolution tools to map photosynthetic metabolism. This knowledge gap has led to the assumption of a hardwired photosynthetic metabolic network[9,10], potentially limiting engineering efforts. Analysing interactions between host metabolism and an engineered non-native pathway using the ethylene-producing cyanobacterium *Synechocystis* sp. PCC 6803 (hereafter *Synechocystis*)[5,11,12] could provide insights on the nature of phototrophic metabolism. Heterologous expression of the Efe allows direct CO_2-to-C_2H_4 conversion via the cyanobacterial TCA cycle, which was perceived as an incomplete pathway with restricted activities[1–4] (Fig. 1). Here we applied isotopically non-stationary ^{13}C metabolic flux analysis (INST-MFA)[13] to wild-type (WT) *Synechocystis* and an ethylene-producing strain. We show global metabolic flux reprogramming towards the engineered ethylene sink, drawing carbon from the TCA cycle. Our results demonstrate a highly flexible metabolic network, supporting efficient CO_2-to-ethylene conversion.

We first constructed and characterized a series of ethylene-producing strains (see Supplementary Methods), all of which were genetically stable. The best strain JU547 harbours the Efe expression cassette with an engineered ribosome binding site (RBS; see Supplementary Methods and File 2). This strain produced 3.8-fold more Efe than the baseline strain JU509 (Fig. 2a) and showed 3.9-fold higher specific ethylene productivity at 718 ± 19 μl l^{-1} h^{-1} per A_{730} (Fig. 2b). Despite high productivity, JU547 displayed identical photosynthetic growth rates as WT and other ethylene-producing strains with a doubling time of 10.7 h, suggesting that ethylene production does not pose a severe metabolic burden that impacts cell growth. We next measured carbon partitioning for ethylene-forming strains. As expected, JU547 diverted the most, 10% of the fixed carbons, to ethylene (Fig. 2b). Based on a recently published flux model[3], this value far surpasses the theoretical maximum of the carbon partitioning ratio (4%, calculated in Supplementary File 3), implying carbon flux is redirected to the engineered ethylene-producing pathway.

To understand the metabolic context of ethylene production in *Synechocystis*, we surveyed the central carbon metabolism in WT using LC–MS that analysed the dynamic incorporation of ^{13}C-labelled nutrients (glucose, bicarbonate and selected amino acids) into downstream metabolites. Feeding uniformly labelled [^{13}C]glucose resulted in rapid and complete labelling of sugar phosphates (Supplementary Fig. 2) with a labelling half-time of 0.5–2 min, suggesting predominant activities of both glycolysis and the pentose phosphate pathway. In comparison, metabolites in the TCA cycle were labelled slowly, indicating limited flux distribution into the cycle. Interestingly, the labelling kinetics of TCA cycle metabolites depend on their locations in the pathway. Those in the right branch (2-oxoglutarate; glutamate, derived directly from 2-oxoglutarate; succinate) exhibited labelling half-times of ≥30 min, whereas the left-branch metabolites (malate; and aspartate, derived directly from oxaloacetate) were labelled more rapidly (labelling half-times of ~4 min). The latter is consistent with the activity of amphibolic reactions that synthesize 4-C metabolites via phosphoenolpyruvate carboxylase and malic enzyme. In agreement with this, the labelling patterns of malate and aspartate are uniform, exhibiting three carbon-labelled forms, likely to be due to fixation of unlabelled CO_2 through carboxylation reactions. These labelled patterns are distinct from those of 2-oxoglutarate and succinate that displayed a dominant appearance of fully labelled isotope, indicative of their genesis from the right branch of the TCA cycle. To further verify this bifurcated architecture of the TCA cycle in photoautotrophic growth, we fed [^{13}C]bicarbonate alone to *Synechocystis* in the light. Again, aspartate exhibited a labelling half-time much shorter than that of succinate (Supplementary Fig. 4), supporting

[1]National Renewable Energy Laboratory, 15013 Denver West Parkway, Golden, Colorado 80401, USA. [2]School of Chemical Engineering, Purdue University, West Lafayette, Indiana 47907, USA. *e-mail: jianping.yu@nrel.gov

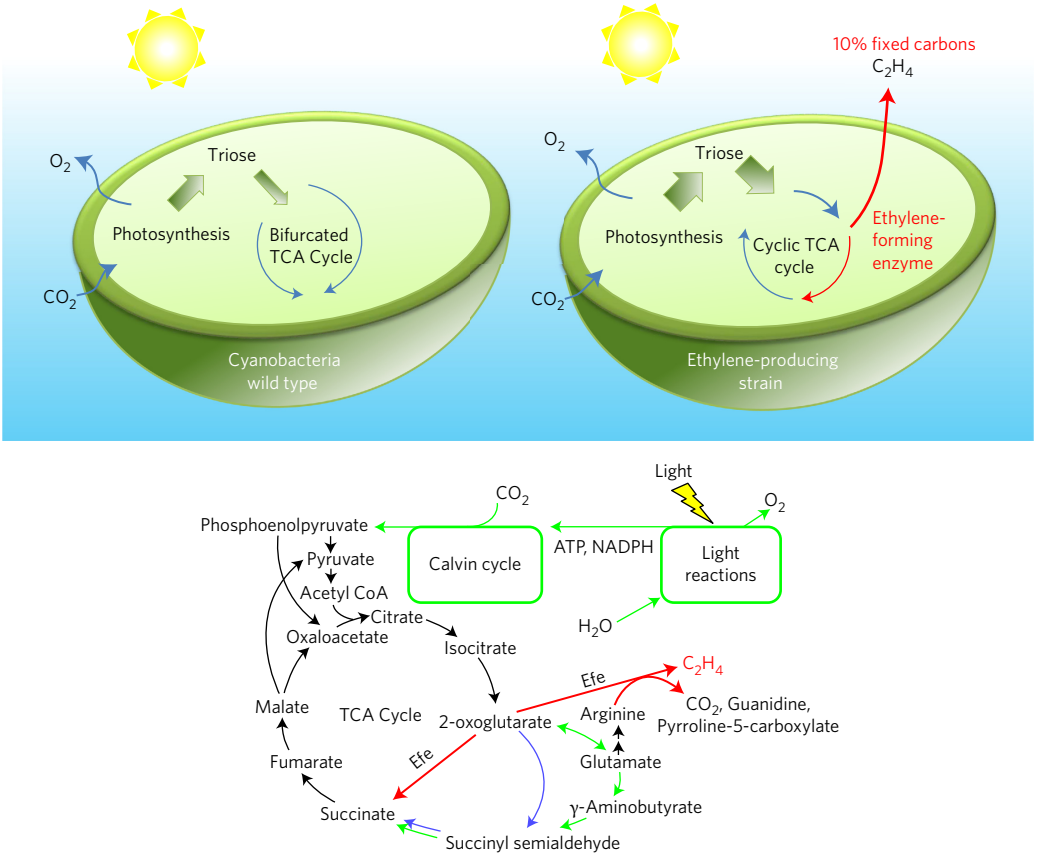

Figure 1 | Ethylene production in a transgenic cyanobacterium. CO_2 to C_2H_4 conversion starts at the Calvin cycle driven by the light reactions of photosynthesis (green boxes). Efe catalyses ethylene production (red arrows) via the TCA cycle (black arrows) recently identified to be closed by the OGDC bypass[26] (blue arrows) and the GABA shunt[27] (green arrows). Ethylene is formed according to the stoichiometric formula[16]: 3 2-oxoglutarate + 3 O_2 + L-arginine → 2 ethylene + succinate + 7 CO_2 + 3 H_2O + guanidine + pyrroline-5-carboxylate.

separating branches of the TCA cycle. Despite the presence of succinate dehydrogenase (Sdh)[14,15], our results indicate that the reaction connecting succinate and fumarate is largely inactive under light conditions.

Efe was proposed to rewire the TCA cycle by converting 2-oxoglutarate to succinate[16]. To investigate how the engineered Efe interacts with the host TCA cycle, we probed the *in vivo* activity of Efe in JU547 by tracing dynamic incorporation of ^{13}C,^{15}N-labelled glutamate into the Efe and the TCA cycle-related metabolites. Labelled glutamate can be taken up by a glutamate transporter[17,18] and converted by glutamate dehydrogenase, generating 2-oxoglutarate that is either metabolized within the TCA cycle or used as a substrate for ethylene production by the heterologous Efe (Fig. 3a). In WT, labelled glutamate quickly appeared in the intracellular pool, followed by rapid labelling of succinate that resulted in 29.1% of succinate labelled in all carbons within 2 min. This labelling ratio remained steady for the rest of the experiment. We also examined the labelling pattern of additional TCA cycle intermediates. However, neither labelled fumarate (data not shown) nor malate (Fig. 3b) was detectable after 30 min. Again, this metabolic discontinuity between succinate and fumarate is consistent with *Synechocysits* harbouring a predominantly bifurcated TCA metabolism in the light. Similarly, a ^{13}C tracer of glutamate to JU547 resulted in rapid appearance of labelled intracellular glutamate, indicating that isotopic glutamate was readily assimilated by the mutant. However, the labelling kinetics of succinate and malate were altered significantly from WT. During a 30-min time course, the ratio of [^{13}C]succinate kept increasing and eventually 56.7% of succinate was labelled in all carbon atoms. This percentage was significantly higher than the 29.1% observed in WT. To exclude the possibility that faster turnover of succinate in JU547 could be due to a smaller pool size, we measured intracellular metabolite concentrations for both strains (Supplementary Table 5). No excreted metabolites were found in significant amounts. The succinate level in JU547 was 0.39 μmol per g dry weight (Fig. 3c), almost double that in WT (0.20 μmol per g dry weight). These data supported that flux from 2-oxoglutarate to succinate was dramatically increased by Efe activity, consistent with its reaction formula (Fig. 1, legend)[16]. We also monitored the labelling of downstream metabolites. Unlike in WT, fully labelled malate, which accounted for 18.9% of the total malate pool, appeared 30 min after glutamate labelling. This observation indicates an altered topology of the TCA cycle in the ethylene-forming strain: instead of a bifurcated architecture, a clockwise cyclic flux proceeds to malate, presumably due to the upregulation of Sdh activity by the increase in succinate levels.

We adapted isotopomer network computational analysis (INCA)[13,19] to quantitatively map photoautotrophic metabolism on the addition of [^{13}C]sodium bicarbonate (Fig. 4a). The identified fluxes with tight error bounds are reliably defined by input of experimental data. In JU547, the measured net carbon fixation rate was 4.3 mmol g^{-1} dry weight h^{-1} a 16% increase over WT (3.7 mmol g^{-1} dry weight h^{-1}; Fig. 4d). These data are consistent with enhanced photosynthetic activity (Fig. 4e; JU547 harboured 19% more chlorophyll *a* per cell and produced O_2 at a rate 19% higher than WT) and increased expenses of energetic co-factors (Fig. 4c; JU547 consumed approximately 14% more ATP and 18% more NADPH than WT). CO_2 influx towards phosphoglycerate formation is diverted: a decreased portion of the flux recycles to drive

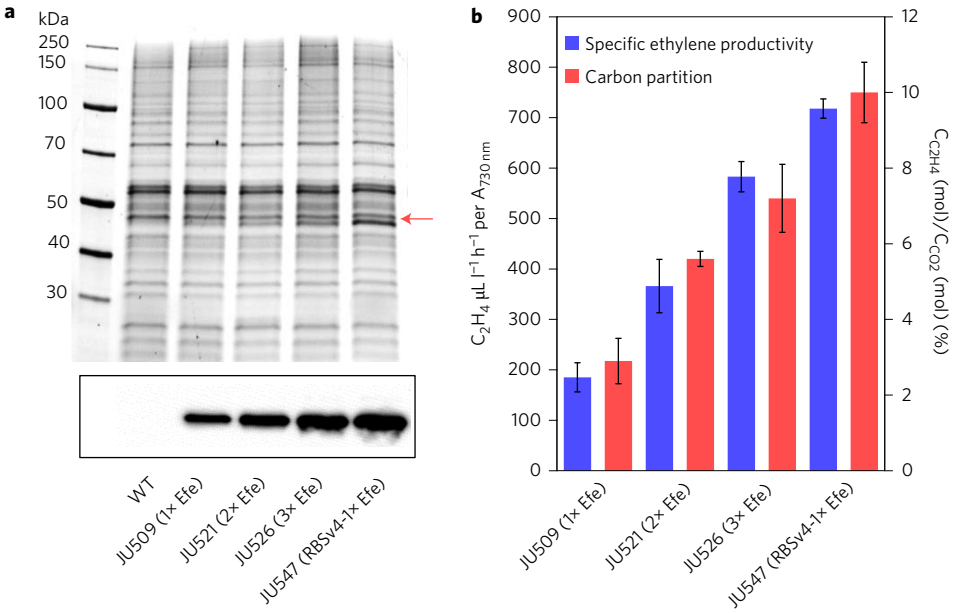

Figure 2 | Efe expression and ethylene productivity. a, SDS–polyacrylamide gel electrophoresis of soluble proteins extracted from *Synechocystis* WT and ethylene producers. Red arrow points to the visible band of Efe, which is also detected by the western blot using the antibody against FLAG-tagged (Asp-Tyr-Lys-Asp-Asp-Asp-Asp-Lys) Efe. **b**, Specific ethylene productivity (left *y*-axis) and carbon partition ratio (right *y*-axis) of ethylene-producing strains (measured under light intensity of 50 μEm^{-2} s^{-1}). Error bars represent biological triplicates.

the carbon fixation cycle, whereas an increased portion is directed downstream towards the TCA cycle and ethylene production. Within the TCA cycle of the ethylene-producing strain (Fig. 4a), the fluxes through the oxidative branch are significantly higher than those in WT. The ethylene producer channelled a higher proportion of total fixed carbon into the TCA cycle via citrate synthase (37% in JU547 versus 13% in WT, Fig. 4d) and absolute fluxes through pyruvate dehydrogenase, citrate synthase, aconitase and isocitrate dehydrogenase were 1.8-, 3.8-, 3.8- and 3.8-fold of corresponding WT values, respectively (Fig. 4b). The production of succinate from 2-oxoglutarate can occur via Efe or succinic semialdehyde dehydrogenase; net fluxes through succinate account for 2.1% CO_2 influx in JU547, and then reach the left branch to form a predominantly cyclic TCA cycle. We also estimated flux ratios in other metabolic nodes that reflect the rigidity of the network structure. Compared with WT, the portion of acetyl coenzyme A directed to the TCA metabolism increased by 117.7% (55.3 versus 25.4%) in the ethylene-producing strain. Unexpectedly, the ratio of enolase to glyceraldehyde 3-phosphate dehydrogenase flux in the distant phosphoglycerate node also increased significantly (12.2 versus 8.8%) in the ethylene-producing strain, suggesting redistribution of global carbon fluxes towards the newly constructed ethylene sink. These data collectively demonstrate metabolic network plasticity in *Synechocystis* in response to a genetic perturbation in the TCA cycle.

In summary, we engineered and characterized an ethylene-producing strain with a synthetic RBS upstream of the *efe* gene and demonstrated improved ethylene production during autotrophic growth. Using ^{13}C-metabolomics techniques we confirmed that Efe serves as a link bridging 2-oxoglutarate and succinate in the TCA cycle, remodels its architecture and increases the carbon flux through the cycle. Overall, this systems-level study uncovers the pathways by which ethylene can be efficiently produced from CO_2 and sunlight in an engineered cyanobacterium, and demonstrated the remarkable plasticity of the metabolic network in response to increased demands for carbon and high-energy molecules that were realized by increased photosynthetic activities and globally redistributed carbon fluxes.

Metabolic engineering towards production of target metabolites requires integration of an engineered biochemical pathway into the metabolic network of the host strains. Therefore, a general principle for metabolic engineering design is to start with pathways that already show high flux so that efforts to strengthen native pathways can be minimized. Accordingly, in cyanobacteria, most efforts have been aimed towards producing compounds (for example sucrose[20], fatty acids[21], alcohol[22,23] and lactate[24]) that are derived from the more active pathways under photosynthetic growth conditions. Although the TCA cycle is a ubiquitous metabolic pathway enabling oxidation of acetyl coenzyme A to CO_2, biosynthesis from the cycle was rarely attempted, presumably because of the common assumption that it is less active in photosynthetic metabolism[25]. In cyanobacteria, the TCA cycle has been perceived to be interrupted between 2-oxoglutarate and succinate because of the absence of a functional 2-oxoglutarate dehydrogenase complex that converts 2-oxoglutarate to succinyl coenzyme A[1,2]. Recent studies supported that the gap between 2-oxoglutarate and succinate may be filled by two independent pathways, the 2-oxoglutarate decarboxylase (OGDC) bypass[26] and the γ-aminobutyrate (GABA) shunt[27] (Fig. 1), although *in vivo* operation of the cycle remains obscure. Indeed, our flux analysis with phototropically grown *Synechocystis* indicates low reaction rates in the TCA cycle, and for the first time provides direct evidence of a bifurcated structure that might barely meet essential growth demands (for example biosynthesis of amino acids such as glutamate, aspartate and arginine). Nevertheless, as hinted by genetic and environmental perturbations on higher plants[28], control of fluxes into the TCA cycle may not be rigid. Here we demonstrate for the first time, in cyanobacteria, that the architecture and fluxes of the TCA cycle were significantly altered towards an engineered ethylene sink. Unexpectedly, these changes redirected 37% of fixed carbons into the cycle and allowed a significant portion (10%) of fixed carbons to channel as ethylene via the cycle, revealing the metabolically malleable nature of this unicellular phototroph. With this new knowledge of metabolic flexibility, the potential of low-flux pathways such as the TCA cycle for cyanobacterial metabolic engineering should be re-evaluated. In addition, the TCA cycle couples to the

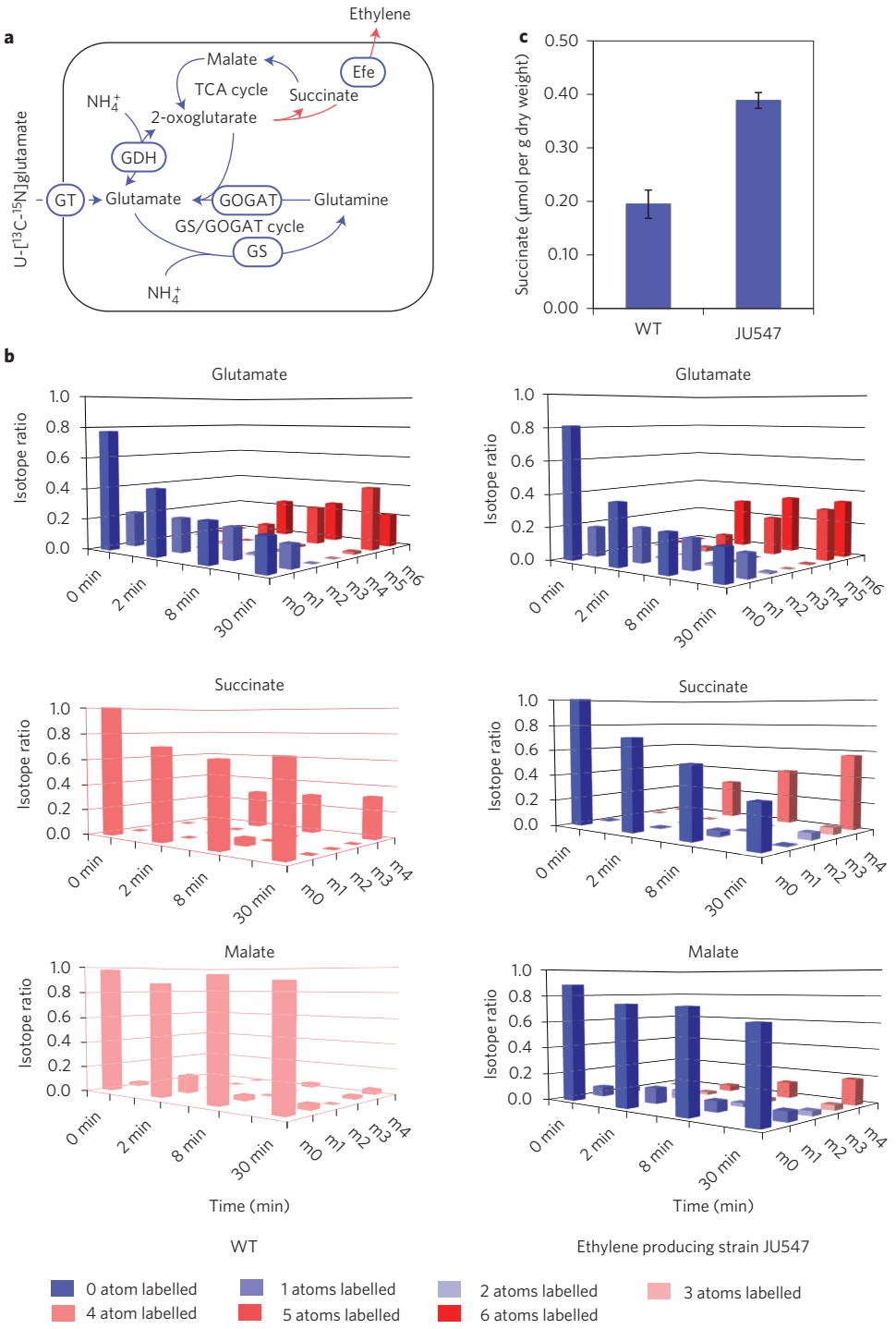

Figure 3 | The TCA cycle fluxes analysed by glutamate labelling. a, Overview of pathways by which uniformly labelled ^{13}C, ^{15}N glutamate is incorporated into metabolites. Labelled glutamate is taken into cells via a glutamate transporter (GT), converted to 2-oxoglutarate by the glutamine synthase/glutamine 2-oxoglutarate aminotransferase (GS/GOGAT) cycle and the glutamate dehydrogenase (GDH), then enters the TCA cycle to form succinate, malate and other TCA metabolites. Succinate can also be formed via the Efe reaction (red arrow, arginine-involved Efe reaction is not shown in this figure). **b**, Dynamic incorporation of U-[^{13}C,^{15}N]glutamate into intracellular glutamate, succinate and malate pool. Comparison of labelling patterns in the WT and the ethylene-producing strain indicates that Efe drives the TCA cycle in a clockwise direction. **c**, Intracellular levels of succinate in WT and JU547 strains. Data presented here indicate results from three biological replicates.

photosynthetic electron transport chain via Sdh, which reduces the plastoquinone pool[14,15] by oxidizing succinate and showed increased flux on ethylene production. Synergistic enhancement of the TCA cycle and photosynthesis supports that targeting respiratory metabolism can be a valid means to improve photosynthesis[29,30].

The above findings raise an intriguing question of why cyanobacteria would preserve such a flexible metabolic network. These organisms are adapted to diurnal cycles in natural environments. When photosynthesis supplies sufficient reducing equivalents and ATP, the TCA cycle maintains low fluxes for biosynthesis. At night the energy demands for cell maintenance are met primarily by

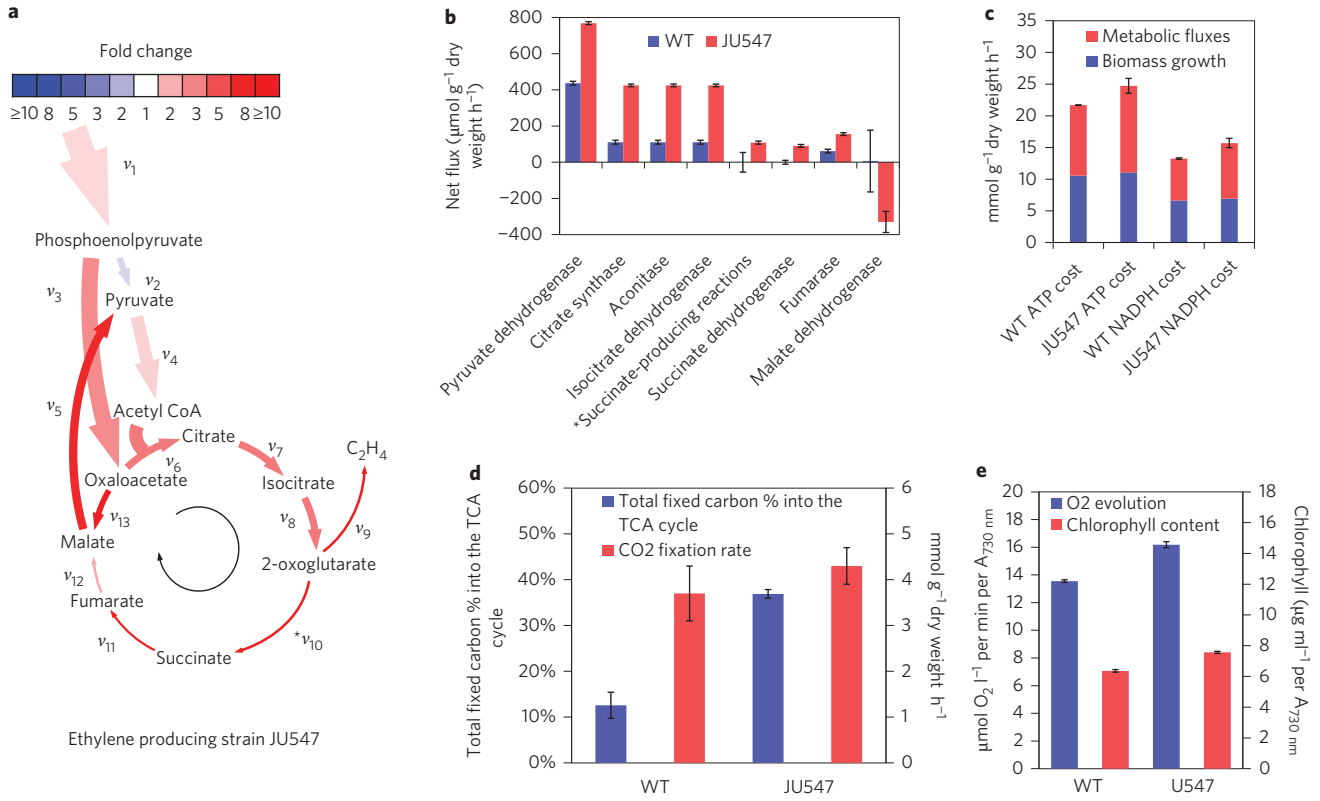

Figure 4 | Comparison of metabolism of *Synechocystis* WT and the ethylene-producing strain JU547. a, Flux map of the TCA cycle and C4 pathways in JU547 made by kinetic ^{13}C flux profiling on [^{13}C]bicarbonate and photoautotrophic growth. Arrow thickness is scaled proportionally to the net flux. The red arrows indicate that the fluxes in JU547 show the increment compared with control fluxes in WT. The blue arrows indicates the opposite. The flux for each reaction is denoted by v_1, enolase; v_2, pyruvate kinase; v_3, phosphoenolpyruvate carboxylase; v_4, pyruvate dehydrogenase; v_5, malic enzyme; v_6, citrate synthase; v_7, aconitase; v_8, isocitrate dehydrogenase; v_9: ethylene forming enzyme, v_{10}: succinate producing reactions, v_{11}: succinate dehydrogenase; v_{12}, fumarase; v_{13}, malate dehydrogenase. Complete fluxomes covering upstream pathways and biomass formation are shown in Supplementary Fig. 3 and Supplementary Fig. 4. **b**, Net fluxes of WT and JU547 in the TCA cycle. *Succinate-producing reactions are those converting 2-oxoglutarate to succinate and include succinic semialdehyde dehydrogenase and Efe. **c**, Net ATP and NADPH consumption in WT and JU547. **d**, CO_2 fixation rate (left *y*-axis) and percentages of total fixed carbons that enter the TCA cycle (right Y axis) in WT and JU547. (Note: $C_{TCA\ cycle}/C_{Total\ fixation} = Flux_{citrate\ synthase} \times 6/(Flux_{Rubisco} + Flux_{PEPC})$. "×6" indicates that citrate, the product of citrate synthase, contains 6 carbons per 1 molecule.) **e**, O_2 evolution rate (left *y*-axis) and chlorophyll *a* content (right *y*-axis) measured for WT and JU547.

respiration, including a more active TCA cycle[27]. Here we show that a photosynthetic cyanobacterium is also endowed with metabolic plasticity, readily adapting to genetic modification of the respiratory pathway. Better understanding of regulation in cyanobacterial metabolism will facilitate further development of photosynthetic biotechnology for renewable production of fuels and chemicals.

Methods

Culture conditions and growth analysis. Unless indicated, all *Synechocystis* strains were grown in BG11 medium (Sigma) supplemented with 20 mM $NaHCO_3$, 4.6 g l^{-1} N-[Tris(hydroxymethyl)methyl]-2-aminoethanesulfonic acid (TES) at 30 °C, and 5% CO_2 under 50 μEm^{-2} s^{-1} illumination from cool white fluorescent lamps, with shaking for liquid cultures or without shaking for plates. For ethylene-forming strains, plates were supplemented with 50 mg l^{-1} spectinomycin and liquid cultures were supplemented with 25 mg l^{-1} spectinomycin. JU521 and JU526 were grown with an additional 200 mg l^{-1} kanamycin. Growth curves were recorded by measuring optical densities at 730 nm with a Beckman DU-630 spectrophotometer. Chlorophyll *a* levels were measured spectrophotometrically in 100% methanol extracts of the cells (1 mg ml^{-1} chlorophyll *a* has an $A_{663\ nm}$ of 82). Whole-chain oxygen evolution rates were measured by a Clark-type electrode (Dissolved Gas Analyzer 1.0, Algae Light and Gas Instruments) at room temperature with a saturating illumination of 2000 μEm^{-2} s^{-1}.

For details of construction of the *Synechocystis* ethylene-producing strains and western blot see the Supplementary Methods.

Ethylene production and carbon partitioning assays. The ethylene production assay was performed as previously described[5]. For carbon partitioning measurements, total CO_2 was calculated as the sum of the dissolved + gaseous CO_2 in a sealed system. Dissolved CO_2 was determined by transferring 2 ml of the culture to a sealed 13 ml Hungate tube and adding 2 ml of concentrated HCl (11.1 M) to release any inorganic carbon out of solution. Headspace gas (500 μl) was then injected into a gas chromatograph to quantify total CO_2. This quantitative approach was validated using blank BG11 medium spiked with known amounts of sodium bicarbonate; the recovery efficiency was ≥95%. Net CO_2 uptake by *Synechocystis* was calculated as the difference between the initial and remaining CO_2 amounts after a period of ethylene production in a sealed tube. A 2:1 molar ratio of CO_2 to ethylene was assumed when calculating the percentage of fixed carbon converted to ethylene.

Dynamic isotope labelling. To perform stable-isotope labelling experiments using labelled substrates (U-[^{13}C]glucose, U-[^{13}C,^{15}N]glutamate and [^{13}C]bicarbonate (Cambridge Isotope Lab, Inc.)), 200 ml aliquots of exponentially growing culture at an $A_{730\ nm}$ of ~1.0 were harvested by centrifugation (4,000 *g* for 10 min) at room temperature. The cell pellets were resuspended and placed into 200 ml of fresh BG11 medium. After 5 min of equilibration, 25 ml of culture was removed and passed through a 47-mm-diameter round hydrophilic nylon filter (Whatman 7408-004 Nylon Membrane 0.8 μm), which was subsequently submerged into 2.0 ml of −80 °C precooled methanol to quench metabolism. Filters remained at −80 °C for at least an hour. Sterile isotopic substrates were then added to the remaining 175 ml of culture (for U-[^{13}C]glucose, U-[^{13}C,^{15}N]glutamate and [^{13}C]bicarbonate, final concentrations were 5 mM, 0.5 mM and 20 mM respectively). Aliquots (25 ml) of labelled cells were removed from the culture, harvested by filtration and subsequently quenched by cold methanol at defined time points (for example 20 s, 1 min, 2 min, 8 min, 30 min) as described above.

Metabolite extraction and LC-MS analysis. See Supplementary Methods.

Data analysis and metabolic flux modelling. See Supplementary Methods.

Received 16 November 2014; accepted 25 March 2015; published online 27 April 2015

References

1. Pearce, J., Leach, C. K. & Carr, N. G. The incomplete tricarboxylic acid cycle in the blue-green alga *Anabaena variabilis*. *J. Gen. Microbiol.* **55,** 371–378 (1969).
2. Smith, A. J., London, J. & Stanier, R. Y. Biochemical basis of obligate autotrophy in blue-green algae and thiobacilli. *J. Bacteriol.* **94,** 972–983 (1967).
3. Young, J. D., Shastri, A. A., Stephanopoulos, G. & Morgan, J. A. Mapping photoautotrophic metabolism with isotopically nonstationary ^{13}C flux analysis. *Metab. Eng.* **14,** 185–185 (2012).
4. You, L., Berla, B., He, L., Pakrasi, B. H. & Tang, Y. J. ^{13}C-MFA delineates the photomixotrophic metabolism of *Synechocystis* sp. PCC 6803 under light- and carbon-sufficient conditions. *Biotechnol. J.* **9,** 684–692 (2014).
5. Ungerer, J. *et al.* Sustained photosynthetic conversion of CO_2 to ethylene in recombinant cyanobacterium *Synechocystis* 6803. *Energ. Environ. Sci.* **5,** 8998–9006 (2012).
6. Sheehan, J. Engineering direct conversion of CO_2 to biofuel. *Nature Biotechnol.* **27,** 1128–1129 (2009).
7. Ducat, D. C., Way, J. C. & Silver, P. A. Engineering cyanobacteria to generate high-value products. *Trends Biotechnol.* **29,** 95–103 (2011).
8. Stephanopoulos, G. & Vallino, J. J. Network rigidity and metabolic engineering in metabolite overproduction. *Science* **252,** 1675–1681 (1991).
9. Melis, A. Carbon partitioning in photosynthesis. *Curr. Opin. Chem. Biol.* **17,** 453–456 (2013).
10. Davies, F. K., Work, V. H., Beliaev, A. S. & Posewitz, M. C. Engineering limonene and bisabolene production in wild type and a glycogen-deficient mutant of *Synechococcus* sp. PCC 7002. *Front. Bioeng. Biotechnol.* **2,** 21 (2014).
11. Guerrero, F., Carbonell, V., Cossu, M., Correddu, D. & Jones, P. R. Ethylene synthesis and regulated expression of recombinant protein in *Synechocystis* sp PCC 6803. *PLoS ONE* **7**, e50470 (2012).
12. Zhu, T., Xie, X. M., Li, Z. M., Tan, X. M. & Lu, X. F. Enhancing photosynthetic production of ethylene in genetically engineered *Synechocystis* sp PCC 6803. *Green Chem.* **17,** 421–434 (2015).
13. Jazmin, L. J. & Young, J. D. Isotopically nonstationary ^{13}C metabolic flux analysis. *Syst. Metab. Eng. Methods Mol. Biol.* **985,** 367–390 (2013).
14. Cooley, J. W., Howitt, C. A. & Vermaas, W. F. J. Succinate: quinol oxidoreductases in the cyanobacterium *Synechocystis* sp strain PCC 6803: presence and function in metabolism and electron transport. *J. Bacteriol.* **182,** 714–722 (2000).
15. Cooley, J. W. & Vermaas, W. F. J. Succinate dehydrogenase and other respiratory pathways in thylakoid membranes of *Synechocystis* sp strain PCC 6803: capacity comparisons and physiological function. *J. Bacteriol.* **183,** 4251–4258 (2001).
16. Fukuda, H. *et al.* Two reactions are simultaneously catalyzed by a single enzyme: the arginine-dependent simultaneous formation of two products, ethylene and succinate, from 2-oxoglutarate by an enzyme from *Pseudomonas syringae*. *Biochem. Biophys. Res. Commun.* **188,** 483–489 (1992).
17. Labarre, J., Thuriaux, P. & Chauvat, F. Genetic analysis of amino acid transport in the facultatively heterotrophic cyanobacterium *Synechocystis* sp strain 6803. *J. Bacteriol.* **169,** 4668–4673 (1987).
18. Quintero, M. J., Montesinos, M. L., Herrero, A. & Flores, E. Identification of genes encoding amino acid permeases by inactivation of selected ORFs from the *Synechocystis* genomic sequence. *Genome Res.* **11,** 2034–2040 (2001).
19. Young, J. D. INCA: a computational platform for isotopically non-stationary metabolic flux analysis. *Bioinformatics* **30,** 1333–1335 (2014).
20. Ducat, D. C., Avelar-Rivas, J. A., Way, J. C. & Silver, P. A. Rerouting carbon flux to enhance photosynthetic productivity. *Appl. Environ. Microb.* **78,** 2660–2668 (2012).
21. Liu, X. Y., Sheng, J. & Curtiss, R. Fatty acid production in genetically modified cyanobacteria. *Proc. Natl Acad. Sci. USA* **108,** 6899–6904 (2011).
22. Deng, M. D. & Coleman, J. R. Ethanol synthesis by genetic engineering in cyanobacteria. *Appl. Environ. Microb.* **65,** 523–528 (1999).
23. Lan, E. I. & Liao, J. C. ATP drives direct photosynthetic production of 1-butanol in cyanobacteria. *Proc. Natl Acad. Sci. USA* **109,** 6018–6023 (2012).
24. Angermayr, S. A., Paszota, M. & Hellingwerf, K. J. Engineering a cyanobacterial cell factory for production of lactic acid. *Appl. Environ. Microb.* **78,** 7098–7106 (2012).
25. Sweetlove, L. J., Beard, K. F. M., Nunes-Nesi, A., Fernie, A. R. & Ratcliffe, R. G. Not just a circle: flux modes in the plant TCA cycle. *Trends Plant Sci.* **15,** 462–470 (2010).
26. Zhang, S. Y. & Bryant, D. A. The tricarboxylic acid cycle in cyanobacteria. *Science* **334,** 1551–1553 (2011).
27. Xiong, W., Brune, D. & Vermaas, W. F. J. The gamma-aminobutyric acid shunt contributes to closing the tricarboxylic acid cycle in *Synechocystis* sp PCC 6803. *Mol. Microbiol.* **93,** 786–796 (2014).
28. Lopez-Bucio, J., Nieto-Jacobo, M. F., Ramirez-Rodriguez, V. & Herrera-Estrella, L. Organic acid metabolism in plants: from adaptive physiology to transgenic varieties for cultivation in extreme soils. *Plant Sci.* **160,** 1–13 (2000).
29. Nunes-Nesi, A. *et al.* Enhanced photosynthetic performance and growth as a consequence of decreasing mitochondrial malate dehydrogenase activity in transgenic tomato plants. *Plant Physiol.* **137,** 611–622 (2005).
30. Nunes-Nesi, A., Araujo, W. L. & Fernie, A. R. Targeting mitochondrial metabolism and machinery as a means to enhance photosynthesis. *Plant Physiol.* **155,** 101–107 (2011).

Acknowledgements

This work is supported by the National Renewable Energy Laboratory Director's Fellowship (W.X.), and the DOE Energy Efficiency and Renewable Energy (EERE) BioEnergy Technologies Office (J.Y., B.W.), EERE Fuel Cell Technologies Office (P.C.M.), and DOE Office of Science BER grant DE-SC0008628 (J.A.M.). We are grateful to Jamey D. Young of Vanderbilt University for providing software and technical assistance on ^{13}C metabolic modelling, and to Maria Ghirardi, Carrie Eckert and William Michener for helpful discussion or assistance with LC–MS equipment.

Author contributions

W.X., J.A.M., P.C.M. and J.Y. conceived the idea, and edited the manuscript. J.U. constructed the strains. B.W. analysed the Efe protein levels. W.X. designed and performed the experiments, analysed data and wrote most of the manuscript.

Additional information

Supplementary information is available online. Reprints and permissions information is available online at www.nature.com/reprints. Correspondence and requests for materials should be addressed to J.Y.

Competing interests

The authors declare no competing financial interests.